ACTA CHEMICA SCANDINAVICA 16 (1962) 327–345

High-Temperature Electrochemical Study of Uranium Oxides in the UO_2 — U_3O_8 Region

KALEVI KIUKKOLA

Metallurgical Laboratory, Institute of Technology, Otaniemi, Finland *

Electromotive force measurements on galvanic cells involving solid electrolytes have been made at temperatures of 800° to 1200°C in order to obtain standard thermodynamic data for the mixing of UO_2 and oxygen gas. Due to the purely anionic conductivity of the electrolyte, a direct evaluation of the relative partial molar free energy of oxygen in uranium oxide as a function of the O/U atomic ratio and temperature has been possible. Therefrom, values for the partial molar heat and entropy of mixing and the corresponding relative integral quantities have been calculated for the whole composition and temperature range investigated. Nonstoichiometry in the homogeneous UO_{2+x} phase is discussed. The solubility of oxygen in this phase was found to be higher than previously known.

In the present investigation, supplementary data to the high-temperature thermodynamic properties of uranium oxides in the UO_2—U_3O_8 region are presented. Following previous suggestions [1,2], an electrochemical technique using galvanic cells with solid electrolytes has been used. The results clarify the phase relations among the stable high-temperature oxide phases and show the dependence of the equilibrium oxygen partial pressure on the composition of the oxide phases or mixtures thereof. Values for the pertinent thermodynamic quantities are evaluated.

In order to obtain the standard molar free energy of formation of uranium oxides with predetermined oxygen-to-uranium ratios, galvanic cells of the previously developed type [3]

$$\mathrm{Fe},\ \mathrm{Fe_xO}\ /\ (0.85\ \mathrm{ZrO_2} + 0.15\ \mathrm{CaO})\ /\ \mathrm{UO_{2+x}}$$

have been investigated. The cell involves at left an iron-wüstite reference electrode with a known equilibrium oxygen partial pressure or the relative partial molar free energy of oxygen. The electrolyte is a solid solution of 85 mole % zirconium dioxide and 15 mole % calcium oxide. Due to its defect

* Present address: Oy Fiskars Ab, Åminnefors, Finland.

structure containing oxygen ion vacancies, this electrolyte is a predominantly anionic conductor over wide variations in the ambient oxygen partial pressure as shown by Kiukkola and Wagner [3] and verified by Kingery *et al.*[4] and Carter [5]. The right-hand electrode is made of uranium oxide with a predetermined oxygen-to-uranium ratio.

EXPERIMENTAL

Uranium oxide electrodes. The various compositions of uranium oxide were prepared in two ways: (1). Reactor grade uranium dioxide powder from Degussa, Germany, was oxidized in air at temperatures below 200°C to the desired overall compositions; (2). Mixtures of UO_3 and U_3O_8 powders, the latter prepared from UO_3 by oxidation in air at 800°C, were heated in evacuated quartz bulbs at 1000°C for about ten days. This method was easier to control.

The prepared uranium oxide powders were pressed into cylindrical pellets of 2 to 3 mm thickness and 8 mm diameter at about 8 ton/cm² pressure. The electrolyte and reference electrode pellets were of the same size. In order to reduce contact with the surrounding atmosphere, the uranium oxide pellets were placed into a cup made of thin platinum foil (Fig. 1). For both types of uranium oxide powders, the final homogenization of the electrodes were performed prior to emf measurements by heating the cell initially to the highest possible measuring temperature (1100 to 1200°C). The method of preparation did not influence the equilibrium oxygen pressure values.

Arrangement of the cell. The apparatus and the arrangement of the cell was similar to that previously described [3]. The same procedure was also followed in the preparation of the electrolyte and the reference electrode.

The cell assembly consisting of the electrolyte tablet between the two electrode tablets (Fig. 1) was inserted into a quartz tube of 26 mm inside diameter placed in a vertical, electrically heated tube furnace. The cell was clamped between two horizontal platinum discs which were provided with platinum connecting leads to the potentiometer. An inert atmosphere was maintained around the cell by flowing a slow stream of argon under a slight overpressure. The gas was purified by passing over silica gel, ascarite and magnesium perchlorate and deoxygenated by passing over active copper at 200°C. Emf measurements were taken with a Rubicon precision potentiometer over the temperature range 800 to 1200°C. A complete temperature cycle was always made. The emf of the Pt, Pt + 10 % Rh thermocouple located near the top electrode was measured with the same potentiometer to ± 1°C. One run lasted from 6 to 30 h.

Each iron-wüstite electrode pellet was used successfully for several experiments. For each run, its surfaces were cleaned with sandpaper. Similar precautions were followed with electrolyte pellets. They were used satisfactorily in one or more experiments.

Analysis of uranium oxides. The oxygen-to-uranium ratios of the electrodes were determined after each run by the usual method of oxidizing the weighed elctrode at about 800°C in air in a platinum boat. The oxidized product is assumed to be $U_3O_{8-\delta}$. It is estimated that this will give the composition to better than the nearest 0.01 atom of oxygen. The change of the composition of the electrodes during an emf experiment was found to be within the analytical accuracy.

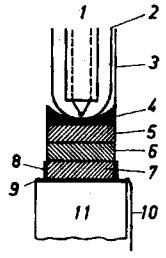

Fig. 1. Cross section of cell with solid electrolyte used in emf measurements. 1. Thermocouple. 2. Quartz tube. 3. Platinum lead. 4. Platinum disc. 5. Reference electrode pellet. 6. Electrolyte pellet. 7. Uranium oxide electrode pellet. 8. Platinum cup. 9. Platinum disc. 10. Platinum lead. 11. Quartz rod.

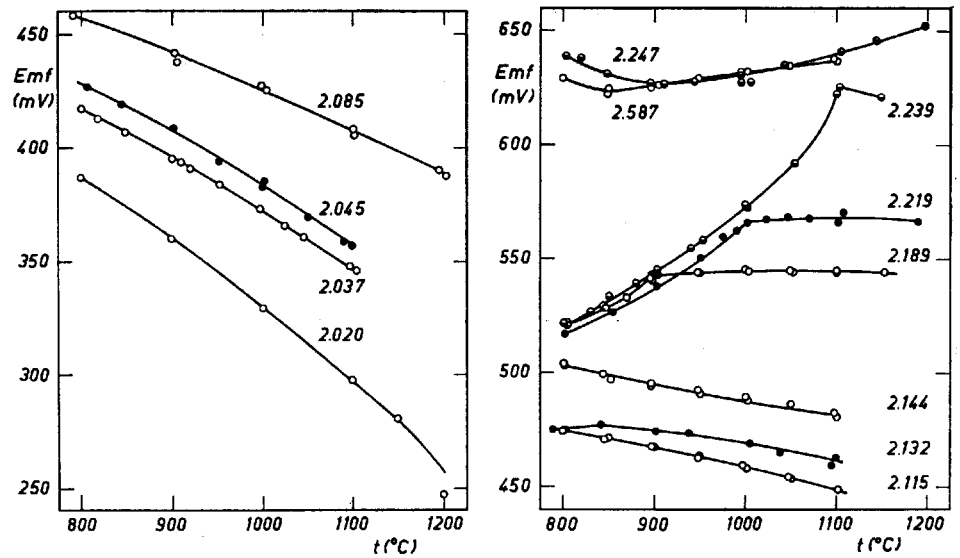

Fig. 2 and 3. Variation of emf of cell Fe, $Fe_xO/(0.85\ ZrO_2 + 0.15\ CaO)/UO_{2+x}$ with temperature for uranium oxides of various O/U atomic ratios.

Solid state coulometric titrations

In addition to the foregoing measurements with uranium oxides of predetermined O/U atomic ratio, a few measurements were performed with the solid state coulometric titration technique developed by Wagner [8,9]. In this method, it is possible to vary the O/U ratio of a given electrode by known amounts and measure the corresponding oxygen partial pressure of the electrode. The galvanic cell was the same as in the other experiments. Prior to measurements, the uranium oxide sample was brought to a composition close to UO_2 by reducing the electrode in hydrogen gas at 1000°C for 4 h and thereafter applying to the assembled cell a positive potential of 0.3 V at 1100°C. The measuring circuit provided instruments for measuring the amount of current passed, the applied potential and the resulting equilibrium potential. All titrations were done at 1100°C to ensure ionic mobility high enough for the homogenization of the electrodes to occur within a reasonable time. For the same reason, the UO_2 electrodes were thin, their weights ranging from 80 to 190 mg.

RESULTS

Electrodes with predetermined composition. Figs. 2 and 3 show plots of emf as a function of composition for some of the uranium oxides with a predetermined O/U atomic ratio. The points shown belong either to descending or ascending temperatures and they deviate from the drawn curves by about $\pm$ 3 mV at most. The emf was found to vary smoothly with temperature at compositions up to $UO_{2.144}$. A definite break in the emf *vs.* temperature curves occurred with the following pellets: $UO_{2.189}$ at about 900°C, $UO_{2.219}$ at about 1000°C, and $UO_{2.239}$ at about 1100°C. These breaks indicate a phase transformation at these temperatures, the homogeneous UO_{2+x} phase prevailing above

these temperatures. The emf values from the composition $UO_{2.250}$ up to $UO_{2.625}$ are practically identical indicating the presence of a two-phase region $UO_{2.250} + UO_{2.667-y}$. Uranium oxide tablets with higher O/U atomic ratio than the above-mentioned, *e.g.* $UO_{2.667}$, gave initially higher emf, too. The final values of emf and composition corresponded to the upper limit of the two-phase region. Due to the high oxygen partial pressures, it was thus impossible to measure the variation of the relative partial molar free energy of oxygen within the $UO_{2.667\pm y}$ one-phase region.

Solid state coulometric titrations. Since the electrolyte is a purely anionic conductor, the passing of current i across the cell during time interval t causes a corresponding transport of oxygen from one electrode to the other. A positive current flowing through the cell from right to left adds oxygen to the UO_2 electrode. The O/U atomic ratio, initially about 2, changes thereby to $2+x$ where x is

$$x = i\,t\,/\,2\,n_U\,F$$

In this equation, n_U is the number of gram atoms of uranium present initially and F is the Faraday constant.

Points of five titrations along with a curve obtained by the conventional method using predetermined electrodes with constant composition are shown in Fig. 4 for the temperature of 1100°C. Due to difficulties in defining the initial composition of the electrodes in titration experiments, it was assumed that they coincided with the conventional curve at a composition defined by their initial emf. The two curves agree at small values of x ($x \leqq 0.2$). At higher O/U ratios, the titrations were not satisfactory presumably due to escape from the uranium oxide electrode of a part of the transported oxygen. It was found that the flow of current, despite its low density, polarized the cell to a potential over 0.9 V which causes oxygen of atmospheric pressure

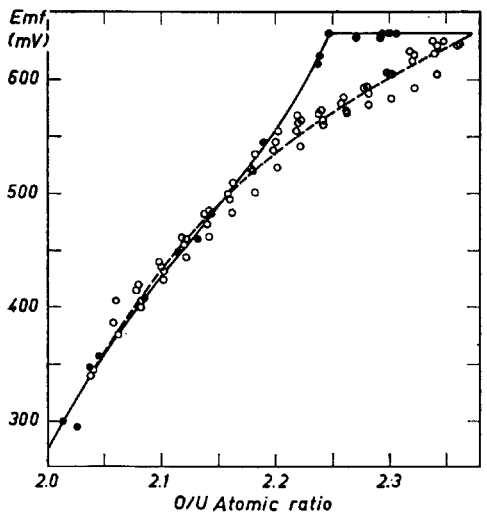

Fig. 4. Variation of emf with uranium oxide composition at 1100°C. —●— measured with cells having predetermined constant composition of uranium oxide, ---O--- experimental points from five coulometric titrations.

Table 1. Relative partial molar free energy of oxygen over iron and wüstite.

	800°C	900°C	1000°C	1100°C	1150°C	1200°C
$\bar{F}_{O_2} - F^{\circ}_{O_2}$ (kcal)	−93.00	−89.76	−86.69	−83.52	−81.96	−80.40

to develop. Diffusion of the transported oxygen into the uranium oxide pellet was evidently too slow. A comparison of the relevant diffusion coefficients [4,10,11] in the various parts of the cell points to the same conclusion. In addition, the phase change of UO_{2+x} to $UO_{2.25}$ may be slow and cause overshooting since the mobility of uranium is very low as pointed out by Wagner [2]. Finally, it was observed that the titrations were amenable to large hysteresis.

For all these reasons, the conventional measurements with predetermined uranium oxide compositions, the only ones reported in the following, were considered more profitable for the present purposes. In the neighborhood of the ideal O/U ratio the titrations may prove useful.

ANALYSIS AND DISCUSSION OF RESULTS

Evaluation of measurements. Since the electrolyte of the cell shows only predominant ionic conduction due to migration of oxygen ions in the electrolyte, the virtual cell reaction may be expressed in terms of oxygen transfer from the right-hand to the left-hand electrode. Hence the emf E of the cell is

$$E = (\bar{F}''_{O_2} - F^{\circ}_{O_2}) - (\bar{F}'_{O_2} - F^{\circ}_{O_2}) / 4F$$

where $\bar{F}'_{O_2}$ and $\bar{F}''_{O_2}$, respectively, are the partial molar free energies of oxygen on the left-hand and the right-hand side of the cell, $\bar{F}^{\circ}_{O_2}$ is the standard molar free energy of oxygen, and F is the Faraday constant. In all experiments made, a mixture of iron and wüstite was used on the left-hand side of the cell. The values for the relative partial molar free energy over iron and wüstite have been evaluated from gas equilibrium measurements [3] and the corrected values are listed in Table 1.

Equilibrium oxygen pressures. Upon substituting the values in Table 1 and the experimental values of E in the above equation, values of the relative partial molar free energy of oxygen,

$$F^{M}_{O_2} = \bar{F}_{O_2} - F^{\circ}_{O_2} = RT \ln p_{O_2},$$

and hence the oxygen partial pressure over uranium oxides can be calculated. The values of the equilibrium oxygen partial pressure as a function of composition are plotted in Fig. 5 at six round temperatures. The corresponding values of the emf were read from large plots of E *vs.* temperature. Fig. 5 includes for comparison some of the data of Biltz and Müller [12] at 1160°C which were determined by a direct manometric measurement. Both type of data agree with

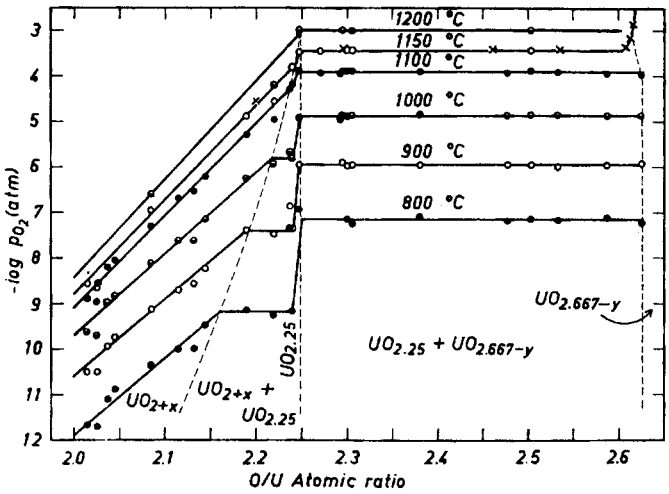

Fig. 5. Variation of equilibrium oxygen pressure with uranium oxide composition at round temperatures between 800°—1200°C. Phase boundaries are indicated with dashed lines. Circles represent data of this study. × represent data of Biltz and Müller [12] at 1160°C.

dan supplement each other very well. The regions were p_{O_2} does not change with composition are two-phase regions. Below $UO_{2.25}$ there is the UO_{2+x} + $UO_{2.25}$ equilibrium and above it the $UO_{2.25}$ + $UO_{2.667-y}$ equilibrium.

The equilibrium oxygen pressures of both two-phase regions are plotted in Fig. 6 as a function of temperature. They are drawn as straight lines which cross at the temperature of 1215° ± 10°C and the log $p_{O_2} = -2.91$. This is the temperature and oxygen pressure above which the UO_{2+x} + $UO_{2.25}$ phase region vanishes (the peritectic point). In the same figure are shown data obtained by Biltz and Müller [12] with manometric pressure measurements, by Blackburn [8] with the Knudsen effusion method, and by Aronson and Belle [13] with the emf method used here. The values of Biltz and Müller for the equilibrium $UO_{2.25}$ + $UO_{2.667-y}$ are in complete agreement with this study. The data of Blackburn are consistently lower. Otherwise, the values are in good agreement.

Phase diagram. Combining the abovementioned facts, it is possible to re-evaluate the usual high-temperature phase diagram for the UO_2 — U_3O_8 range (Fig. 7). In particular, the diagram shows the solubility of oxygen in the UO_{2+x} phase and compares it with the previous evaluations by Grønvold [6], Blackburn [8], Aronson and Belle [13], and Willardson *et al.*[14]. The experimental evidence of Aronson and Belle is fully confirmed. It thus seems established that the solubility of oxygen in the UO_{2+x} phase is greater than is usually shown on phase diagrams which are mainly based on the works by Grønvold and Blackburn.

The $UO_{2.25}$ phase is shown schematically as a straight line since its boundaries are still too inaccurate. The uppper boundary of the $UO_{2.25}$ + $UO_{2.667-y}$

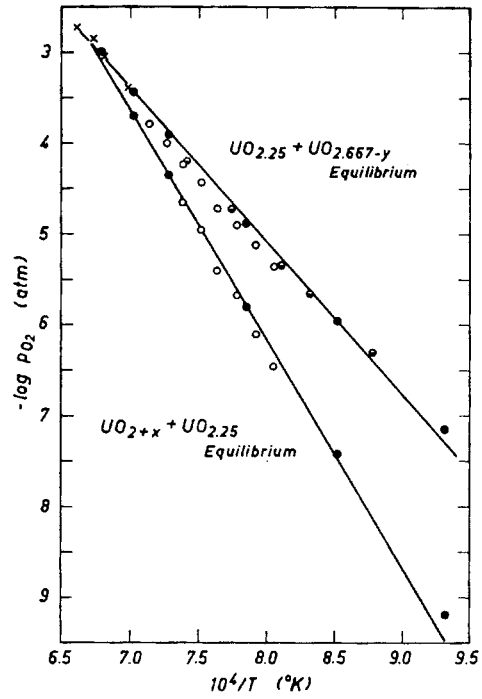

Fig. 6. Plot of log p_{O_2} *vs.* $1/T$ for UO_{2+x} + $UO_{2.25}$ and $UO_{2.25}$ + $UO_{2.667-y}$ equilibria. —●— this study, O Blackburn [8], × Biltz and Müller [12], ◒ Aronson and Belle [13].

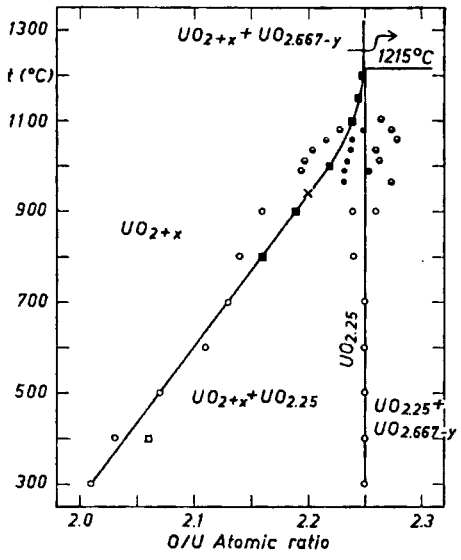

Fig. 7. Phase diagram for the range UO_2 — $UO_{2.3}$. —■— this study, O Gronvold [6], × Aronson and Belle [13], ● & ◒ Blackburn [8], □ Willardson *et al.*[14].

phase field is estimated to be at around $UO_{2.625}$ between 800°—1100°C and, according to Biltz and Müller [12], at around $UO_{2.61}$ above this temperature range. The peritectic temperature, above which the miscibility gap between the phases UO_{2+x} and $UO_{2.25}$ disappears, was estimated by Belle and Auskern [10] to be around 1170°C. A complete miscibility at higher temperatures was inferred by Grønvold [6] from crystallographic considerations.

Integral molar free energies. Choosing the components in uranium oxide of any composition as UO_2 and O_2, then the composition of the oxide is determined by the mole fraction N_{UO_2} or N_{O_2}. If the O/U atomic ratio in the oxide is $2+x$, where $0 \leqq x \leqq 1$, then $N_{UO_2} = 2/(2+x)$ and $N_{O_2} = x/(2+x)$. With the help of the measured values of the relative partial molar free energy of oxygen, $F^M_{O_2}$, it is possible to calculate the relative integral molar free energy F^M for the formation of uranium oxide of any composition from the UO_2 of ideal composition and oxygen gas from the formula [15]

$$F^M = (1-N_{O_2}) \int_0^{N_{O_2}} \frac{F^M_{O_2}}{(1-N_{O_2})^2} \, dN_{O_2}$$

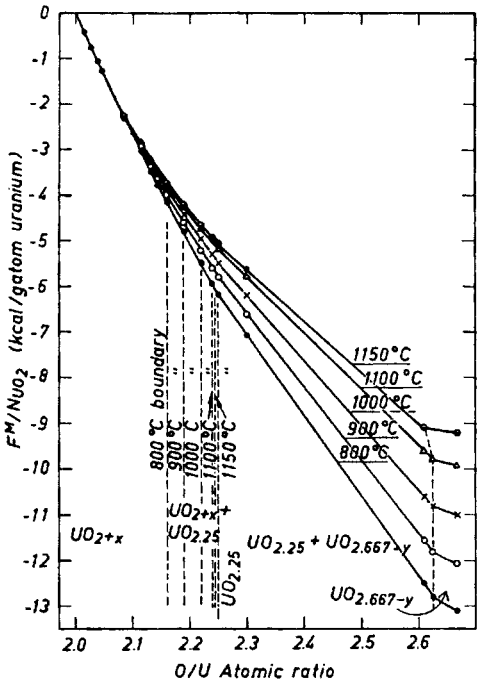

Fig. 8. Integral free energy of formation of uranium oxide from UO_2 and O_2 per gram atom uranium as a function of composition at five round temperatures. Phase boundaries are indicated by dashed lines.

The evaluation of this integral was done graphically in the homogeneous regions and numerically in the two-phase regions where $F^M_{O_2}$ is constant. It was assumed that the phase diagram is of the form shown in Fig. 7 with the phase $UO_{2.25}$ having a very narrow region of homogeneity. The oxygen pressure data for the $UO_{2.667-y}$ phase were estimated from the measurements by Biltz and Müller [12]. Fig. 8 shows the variation with composition of F^M/N_{UO_2}, *i.e.* the relative integral molar free energy per gram atom uranium for five round temperatures, the values for 1200°C being very close to those shown for 1150°C. Table 2 includes a complete list of all thermodynamic data.

Relative partial molar heat of solution of oxygen in uranium oxide. This quantity,

$$H^M_{O_2} = \bar{H}_{O_2} - H^\circ_{O_2}$$

where $H^M_{O_2}$ is the partial molar enthalpy of oxygen gas and $H^\circ_{O_2}$ is the standard molar enthalpy of oxygen gas, is obtained readily from the temperature coefficient of the oxygen pressure at constant composition provided the oxide solution is homogeneous over the whole temperature range. The previously given values of $\log p_{O_2}$ were plotted against $1/T$ at constant compositions within the UO_{2+x} phase region. The resulting curves were essentially straight over the temperature range covered. Their slope multiplied by 4.575 gives $H^M_{O_2}$

Table 2. Variation of the thermodynamic properties of uranium oxides with composition and temperature.

O/U atomic ratio	Temp. °C	Relative partial quantities $-H^M_{O_2}$ kcal	$-F^M_{O_2}$ kcal	$-S^M_{O_2}$ e.u.	Relative integral quantities $-H^M/N_{UO_2}$ kcal	$-F^M/N_{UO_2}$ kcal	$-S^M/N_{UO_2}$ e.u.
2.014	800	59.9	57.30	2.39	0.42	0.41	0.01
	900	59.9	56.46	2.90	0.42	0.40	0.01
	1000	59.9	56.06	2.99	0.42	0.40	0.02
	1100	59.9	55.84	2.93	0.42	0.39	0.02
	1150	59.9	55.76	2.88	0.42	0.39	0.02
2.026	800	59.8	57.48	2.15	0.78	0.76	0.02
	900	59.8	56.46	2.84	0.78	0.74	0.04
	1000	59.8	56.48	2.60	0.78	0.73	0.04
	1100	59.8	56.31	2.53	0.78	0.74	0.03
	1150	59.8	56.41	2.38	0.78	0.74	0.03
	1200	59.8	57.6	1.5	0.78	0.75	0.02
2.037	800	63.7	54.53	8.57	1.12	1.07	0.05
	900	63.7	53.27	8.92	1.12	1.04	0.07
	1000	63.7	52.37	8.92	1.12	1.03	0.07
	1100	63.7	51.51	8.90	1.12	1.04	0.06
2.045	800	62.3	53.42	8.23	1.38	1.28	0.09
	900	62.3	52.26	8.52	1.38	1.25	0.10
	1000	62.3	51.36	8.55	1.38	1.24	0.11
	1100	62.3	50.59	8.49	1.38	1.25	0.10
2.085	800	66.6	50.84	14.7	2.70	2.32	0.35
	900	66.6	48.98	15.0	2.70	2.26	0.37
	1000	66.6	47.30	15.2	2.70	2.23	0.37
	1100	66.6	45.93	15.1	2.70	2.22	0.35
	1150	66.6	45.24	15.0	2.70	2.21	0.34
	1200	66.6	44.51	15.0	2.70	2.21	0.33
2.115	800	74.1	49.23	23.2	3.67	3.03	0.60
	900	74.1	46.68	23.4	3.67	2.93	0.63
	1000	74.1	44.35	23.4	3.67	2.88	0.62
	1100	74.1	42.10	23.3	3.67	2.84	0.61
2.132	800	74.8	49.13	23.9	4.35	3.49	0.80
	900	74.8	45.99	24.5	4.35	3.37	0.84
	1000	74.8	44.35	23.9	4.35	3.29	0.83
	1100	74.8	41.08	24.5	4.35	3.23	0.82
2.144	800	73.3	46.55	24.9	4.89	3.78	1.04
	900	73.3	44.14	24.9	4.89	3.64	1.07
	1000	73.3	41.67	24.8	4.89	3.55	1.06
	1100	73.3	39.05	24.9	4.89	3.46	1.04
2.160	800	—[a]	45.11	—[a]	5.38	4.15	1.15
	900	74.8	42.50	27.5	5.38	4.00	1.18
	1000	74.8	39.78	27.5	5.38	3.87	1.18
	1100	74.8	36.94	27.6	5.38	3.76	1.18
	1150	74.8	35.48	27.6	5.38	3.74	1.15

Table 2. Continued.

2.189	800	116.1	44.94	66.4	7.06	4.80	2.11
	900	—[a]	39.67	—[a]	6.48	4.59	1.62
	1000	77.4	36.41	32.2	6.48	4.43	1.62
	1100	77.4	33.24	32.1	6.48	4.27	1.61
	1150	77.4	31.77	32.0	6.48	4.21	1.60
2.219	800	116.1	45.35	66.0	8.81	5.48	3.10
	900	116.1	40.22	64.7	8.22	5.20	2.57
	1000	—[a]	34.57	—[a]	7.60	4.96	2.07
	1100	71.9	31.12	29.7	7.60	4.73	2.09
	1150	71.9	29.65	29.7	7.60	4.65	2.07
	1200	71.9	28.14	29.7	7.60	4.51	2.10
2.239	800	116.1	45.03	66.3	9.97	5.93	3.76
	900	116.1	39.57	65.3	9.39	5.58	3.24
	1000	116.1	33.83	64.7	8.76	5.30	2.72
	1100	—[a]	26.23	—[a]	8.31	5.03	2.39
	1150	69.7	24.67	31.6	8.31	4.92	2.39
2.245	1150	—[a]	24.09	—[a]	8.52	5.00	2.44
2.248	1200	—[a]	21.03	—[a]	8.62	4.87	2.55
2.250	800	—	35.12	—	10.6	6.18	4.13
	900	—	31.97	—	10.0	5.80	3.60
	1000	—	28.41	—	9.40	5.49	3.07
	1100	—	24.57	—	8.95	5.18	2.75
	1150	—	22.36	—	8.81	5.06	2.63
	1200	—	20.17	—	8.74	4.90	2.60
2.300	800	77.1	35.12	39.1	12.5	7.06	5.10
	900	77.1	31.97	38.5	12.0	6.60	4.56
	1000	77.1	28.41	38.2	11.3	6.20	4.03
	1100	77.1	24.57	38.2	10.9	5.79	3.70
	1150	77.1	22.36	38.5	10.7	5.62	3.59
	1200	77.1	20.17	38.7	10.7	5.40	3.58
2.610	1150	—[b]	22.36	—[b]	22.7	9.09	9.55
	1200	—[b]	20.17	—[b]	22.6	8.52	9.56
2.625	800	—[b]	35.12	—[b]	25.1	12.80	11.4
	900	—[b]	31.97	—[b]	24.5	11.80	10.8
	1000	—[b]	28.41	—[b]	23.9	10.81	10.2
	1100	—[b]	24.57	—[b]	23.4	9.78	9.92
2.667	800	50	— 2.5	49	26.2	13.08	12.2
	900	50	— 5.5	47	25.6	12.02	11.6
	1000	50	— 8.4	46	25.0	11.00	11.0
	1100	50	—11.3	45	24.6	9.90	10.7
	1150	50	—12.8	44	24.3	9.19	10.6
	1200	50	—14.3	44	24.3	8.60	10.6

[a] Solubility limit of the UO_{2+x} phase
[b] Upper boundary of the $UO_{2.25}$ + $UO_{2.667-y}$ phase region

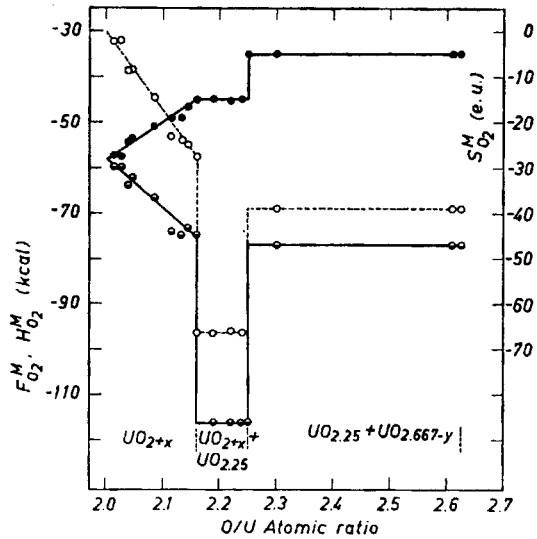

Fig. 9. Variation with uranium oxide composition of relative partial molar free energy $F^M_{O_2}$ (—●—), partial molar heat of mixing $H^M_{O_2}$ (—◒—), and partial molar entropy of mixing $S^M_{O_2}$ (---O---), respectively. Temperature is 800°C.

which is shown as a function of composition in Fig. 9 for the temperature of 800°C. Fig. 9 shows also values for $F^M_{O_2}$, The detailed data are listed in Table 2.

The relative partial molar heat of addition of oxygen increases about linearly with the O/U ratio within the homogeneous UO_{2+x} phase. The appearance of the stable intermediate phase $UO_{2.25}$ causes a large drop in $H^M_{O_2}$ for the two-phase region UO_{2+x} + $UO_{2.25}$. For the second two-phase region $UO_{2.25}$ + $UO_{2.667-y}$ the partial heat of solution is again larger, *i.e.* of the same order of magnitude as at the saturation limit of the UO_{2+x} phase. The evaluation of the partial heats of solution for the two-phase regions is considered later in this paper.

Relative partial molar entropy of oxygen. This quantity,

$$S^M_{O_2} = \bar{S}_{O_2} - S^\circ_{O_2}$$

where $\bar{S}_{O_2}$ is the partial molar entropy of oxygen and $S^\circ_{O_2}$ is the standard molar entropy of oxygen, is obtained from the values of $F^M_{O_2}$ and $H^M_{O_2}$ by the formula

$$S^M_{O_2} = (H^M_{O_2} - F^M_{O_2}) / T$$

The values for 800°C are shown in Fig. 9 and the detailed data are listed in Table 2. The behavior is similar to $H^M_{O_2}$ with a large drop in the UO_{2+x} + $UO_{2.25}$ phase region. Likewise, the partial molar entropies are practically independent of temperature if phase transformations are excluded.

The results are tentatively interpreted to indicate a continuous increase of order in the oxygen sublattice with the dissolution of oxygen in the UO_{2+x} phase. A pronounced increase of order leading to a more stable configuration of atoms is achieved by the transformation of the saturated UO_{2+x} phase to the $UO_{2.25}$ phase. The decrease in the enthalpy, $H^M_{O_2}$, due to the phase transformation is greater than the corresponding change in the subtractive term, $T\,S^M_{O_2}$, of the free energy equation. At higher temperatures the subtractive term, enthalpies and entropies being essentially independent of temperature, becomes the more important and the phase $UO_{2.25}$ tends therefore to grow unstable. The critical point is the peritectic temperature.

In the above qualitative discussion, changes in the electronic consititution of the oxide have not been considered. A simplified treatment of the dependence of the O/U ratio and the concentrations of the individual ionic and electronic lattice defects in the homogeneous UO_{2+x} phase on the oxygen partial pressure of the surrounding gas is presented in the last part of this paper.

All the relative partial quantities of this investigation are at least in fair agreement with the previously published data [8,13].

Relative integral molar heat of mixing. By performing an integration analogous to the one for F^M, it is possible to obtain from the partial heats of mixing the relative integral molar heat of reaction, H^M, of UO_2 and O_2 for the whole composition range studied. In Table 3 results of such evaluations are presented for F^M/N_{UO_2} and H^M/N_{UO_2} at the solubility limit of the phase UO_{2+x}. Included are also the values of $F^M_{O_2}$ for the both two-phase equilibria. Within the UO_{2+x} phase region the integral heat of reaction per mole O_2, *i.e.* H^M/N_{O_2}, is of the same order of magnitude as the relative partial molar heat of addition of oxygen.

In order to obtain the values of H^M beyond the solubility limit of the homogeneous UO_{2+x} phase, it is necessary to evaluate the heat of the equilibrium reaction when 1 gram mole of O_2 reacts with UO_{2+x} to form $UO_{2.25}$ both solid phases being of the appropriate equilibrium compositions. Similarly, it is needed the corresponding heat of the equilibrium reaction for oxygen

Table 3. Relative integral free energy F^M/N_{UO_2} and relative integral heat of mixing H^M/N_{UO_2} per gram atom uranium at the solubility limit of the UO_{2+x} phase. Relative partial molar free energies of oxygen $F^M_{O_2}$ for the two-phase equilibria UO_{2+x} + $UO_{2.25}$ and $UO_{2.25}$ + $UO_{2.667-y}$.

Temp. °C	Solubility limit(O/U)	F^M/N_{UO_2} kcal	H^M/N_{UO_2} kcal	$F^M_{O_2}$ $(UO_{2+x}+UO_{2.25})$ kcal	$F^M_{O_2}$ $(UO_{2.25}+UO_{2.667-y})$ kcal
800	2.160	−4.15	−5.38	−45.11	−35.12
900	2.189	−4.59	−6.48	−39.82	−31.97
1000	2.219	−4.96	−7.60	−33.80	−28.41
1100	2.239	−5.03	−8.31	−27.32	−24.57
1150	2.245	−5.00	−8.52	−24.09	−22.36
1200	2.248	−4.9	−8.6	−21.0	−20.17

and $UO_{2.25}$ forming the $UO_{2.667-y}$ phase. Both values are readily obtained from the slopes of the lines in Fig. 6 which show the two two-phase equilibrium oxygen pressures as a function of temperature.

For the reaction

$$UO_{2+x} + (0.125 - x/2)\, O_2 = UO_{2.25}$$

the heat of reaction per 1 gram mole O_2 is thus -116.1 kcal. For the other equilibrium reaction

$$UO_{2.25} + (0.209 - y/2)\, O_2 = \overline{UO_{2.667-y}}$$

the heat of reaction per gram mole O_2 is -77.1 kcal. Biltz and Müller's[12] results for the same reaction measured in the temperature range 1160—1240°C give about -85 kcal/mole O_2. Blackburn [8] obtained in the range 966—1126°C a value of -78.2 kcal/mole O_2.

With the help of these values and by taking into account the actual amounts of the reacting O_2, it is possible to calculate the H^M-values over the whole range investigated. Finally, it is possible to calculate $H^M_{O_2}$ at any point, especially for the two-phase regions, from the formula [15]

$$H^M_{O_2} = H^M + (1 - N_{O_2})\left(\frac{\partial H^M}{\partial N_{O_2}}\right)$$

The calculated values are listed in Table 2. Values for the $UO_{2.667-y}$ phase region were estimated from Biltz and Müller's [12] results. It is interesting to note that the relative partial molar heats of addition of oxygen for the both two-phase regions are practically as large as the heats of reaction for the corresponding equilibrium reactions.

A plot of H^M/N_{UO_2} *vs.* O/U atomic ratio is of the same shape as for the free energy in Fig. 8.

Relative integral molar entropy of mixing. The values of this quantity, S^M, were evaluated from the values for H^M and F^M by the usual formula. Results are listed in Table 2. A plot of S^M/N_{UO_2} *vs.* O/U ratio is of the same shape as for the free energy in Fig. 8.

Further comparison of the high-temperature thermodynamic results. Fig. 10 shows the standard free energy change as a function of temperature for the reactions

$$UO_2 + 0.125\, O_2 = \overline{UO_{2.25}}$$

and

$$UO_2 + 0.333\, O_2 = UO_{2.667}$$

The values of Coughlin [16] for the last reaction are about 1.5 kcal less negative. Blackburn's [8] evaluation at 1300°K is in good agreement. A recent evaluation by Ackermann [17] differs markedly only at higher temperatures.

Fig. 11 shows the corresponding standard heats of reaction. The agreement to other evaluations is fairly good.

Extrapolation of the high-temperature results to 25°C. By a straight line extrapolation of the high-temperature free energy values for the reaction

$$UO_2 + 0.125\, O_2 = UO_{2.25}$$

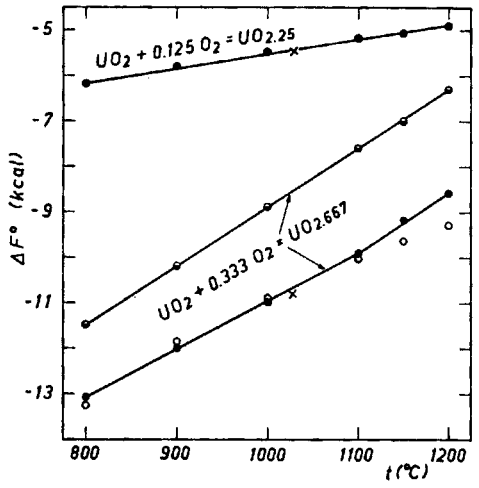

Fig. 10. Variation with temperature of standard free energy change of the reactions $UO_2 + 0.125\ O_2 = UO_{2.25}$ and $UO_2 + 0.333\ O_2 = UO_{2.667}$. —●— this study, × Blackburn [8], ◒ Coughlin [16], O Ackermann [17].

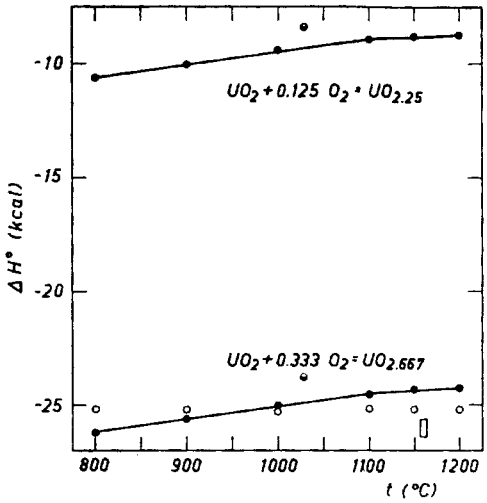

Fig. 11. Variation with temperature of the standard heats of reaction for $UO_2 + 0.125\ O_2 = UO_{2.25}$ and $UO_2 + 0.333\ O_2 = UO_{2.667}$. —●— this study, ◒ Blackburn [8], O Coughlin [16], □ Biltz and Müller [12].

to 25°C one obtains $\Delta F°_{298} = -8.57$ kcal. The standard molar entropies at 25°C are: UO_2 18.623 e.u.[18]; O_2 49.003 e.u.[19]; $UO_{2.25}$ 20.073 e.u.[20]. Thus $\Delta S°_{298} = -4.675$ e.u. and combining this with the extrapolated free energy value one obtains $\Delta H°_{298} = -9.96$ kcal or -79.7 kcal/mole O_2. The corresponding values according to Brewer's [21] estimations are: $\Delta F°_{298} = -9.9$ kcal and $\Delta H°_{298} = -10.8$ kcal or -86.4 kcal/mole O_2.

By a similar extrapolation of the present high-temperature free energy values for the reaction

$$UO_2 + 0.333\ O_2 = UO_{2.667}$$

to 25°C one obtains $\Delta F°_{298} = -21.31$ kcal. The standard molar entropy at 25°C for $UO_{2.667}$ is 22.511 e.u.[22]. The standard entropy change of this reaction is thus $\Delta S°_{298} = -12.446$ e.u. Huber *et al.*[23] have determined the standard heat of the reaction calometrically at 25°C and obtained a value $\Delta H°_{298} = -25.34$ kcal. Combining this value with the standard entropy change one obtains $\Delta F°_{298} = -21.63$ kcal in satisfactory agreement with the extrapolated result of this research.

Using the oxygen pressure data of Biltz and Müller [12] at 580°C and in the composition range $UO_{2.667} - UO_3$ one can evaluate as before for the reaction

$$UO_{2.667} + 0.167\ O_2 = UO_3$$

$\Delta F^\circ_{853} = -160$ cal and $\Delta H^\circ_{853} = -7.5$ kcal. Combining these values with the linearly extrapolated high-temperature results of this study for the reaction

$$UO_2 + 0.333\ O_2 = UO_{2.667}$$

one obtains for the reaction

$$UO_2 + \tfrac{1}{2}\ O_2 = UO_3$$

$\Delta F^\circ_{853} = -15.6$ kcal and $\Delta H^\circ_{853} = -33.7$ kcal. The same quantities according to Coughlin [16] are: $\Delta F^\circ_{853} = -15.3$ kcal and $\Delta H^\circ_{853} = -31.8$ kcal. Upong using the enthalpy and entropy increments of UO_2, O_2, and UO_3 between 298° and 853°K as compiled by Kelley [24], the following values are obtained for the last reaction: $\Delta F^\circ_{298} = -28.5$ kcal and $\Delta H^\circ_{298} = -33.7$ kcal. The corresponding values according to Coughlin [16] are: $\Delta F^\circ_{298} = -25.9$ kcal and $\Delta H^\circ_{298} = -31.8$ kcal.

High-temperature heat-content and entropy data. Upon combining the high-temperature results of this study with the high-temperature heat-content and entropy data for UO_2 and O_2 as compiled by Kelley [24] and the necessary values of ΔH°_{298} and ΔS°_{298} mentioned above, one can evaluate high-temperature heat-content and entropy data for the compounds $UO_{2.25}$ and $UO_{2.667}$ (Table 4). Westrum and Grønvold [22] have determined the heat content of $UO_{2.667}$ over the range from 5° to 350°K. Popov *et al.*[25] have measured the heat capacity of the same compound over the ranges of 100—320°C and 400—600°C. Combining these two investigations and extrapolating the latters' results one obtains for $UO_{2.667}$ the value $H_{1000} - H_{298} = 18.0$ kcal or much higher than the value 13.8 kcal of the present evaluation. The heat capacity values of Popov for UO_3 are also greater than those of Kelley [24].

Non-stoichiometry in uranium dioxide. Wagner [2] has formulated equations for the equilibria of lattice defects in low concentrations within a single phase UO_{2+x} or with a gaseous phase O_2 in terms of the classical law of mass action. The following theoretical relations for the dependence of the oxygen-to-uranium ratio and the concentrations of the individual lattice defects on the oxygen partial pressure of the surrounding gas show the essential results.

Table 4. High-temperature heat content and entropy data for $UO_{2.25}$ and $UO_{2.667}$.

	$UO_{2.25}$		$UO_{2.667}$	
T °K	$H_T - H_{298}$ kcal/mole	$S_T - S_{298}$ e.u.	$H_T - H_{298}$ kcal/mole	$S_T - S_{298}$ e.u.
1000	12.9	23.7	13.8	25.6
1100	15.6	26.3	16.7	28.0
1200	18.4	28.7	19.7	30.7
1300	21.2	30.9	22.6	33.1
1400	23.8	32.9	25.5	35.2
1473	25.6	34.1	27.4	36.4

Assuming that the concentration of interstitial cations and cation vacancies are negligible and disregarding associated lattice defects, it follows from elementary stoichiometry that

$$x - X_O - X_\square = \tfrac{1}{2} X_p - \tfrac{1}{2} X_n \quad (1)$$

where x is the excess of oxygen per uranium ion in oxide of the overall composition UO_{2+x}. X_O, $X_\square$, X_p, and X_n are the ratios of the numbers of interstitial oxygen ions, oxygen ion vacancies, electron holes, and excess electrons to the number of uranium atoms, respectively. These are the principal lattice defects considered.

Electronic defects within the UO_2 phase are created by the reaction

$$\text{electron in valence band} = \text{excess electron} + \text{electron hole} \quad (2)$$

with the equilibrium condition

$$X_n X_p = K_1 \quad (3)$$

The excess oxygen in UO_{2+x} results from the addition of oxygen ions into interstitial positions according to the following reaction between gaseous oxygen and solid UO_2,

$$\tfrac{1}{2} O_2(g) + 2 \text{ electrons in valence band} = \text{interstitial oxygen ion} + 2 \text{ electron holes} \quad (4)$$

with the equilibrium condition

$$X_O X_p^2 / p_{O_2}^{\frac{1}{2}} = K_2 \quad (5)$$

For a uranium oxide with the O/U atomic ratio $\geqq 2$, we may assume that $X_\square \cong 0$. Eqn. (1) becomes then simply

$$x \cong X_O \quad (6)$$

Eqn. (5) yields

$$x = K_2 X_p^{-2} p_{O_2}^{\frac{1}{2}} \quad (7)$$

Two limiting cases are considered. (I) Assume that the oxygen excess, x, is much less than the concentrations of the electronic defects in UO_2 of ideal composition, *i.e.*

$$x \ll K_1^{\frac{1}{2}} \quad (8)$$

Hence

$$X_p \cong X_n \cong K_1^{\frac{1}{2}} \quad (9)$$

From eqn. (7) it follows that

$$x = \overline{K_1^{-1} K_2}\, p_{O_2}^{\frac{1}{2}} \quad (10)$$

Thus under conditions where the concentrations of electronic defects are large in the stoichiometric oxide and the variations of these concentrations with changes in degree of non-stoichiometry is small, the amount of oxygen excess should be linearly proportional to the square root of the ambient oxygen partial pressure.

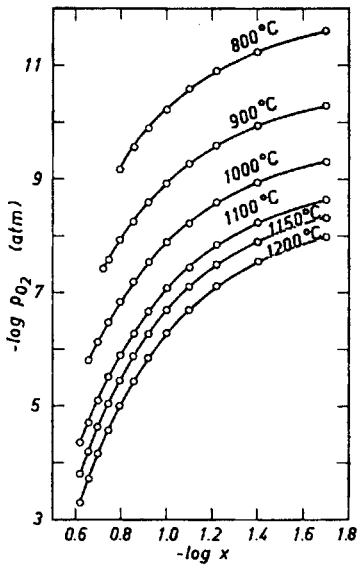

Fig. 12. Change of log p_{O_2} with log x at round temperatures within the UO_{2+x} phase.

(II) Assume an excess of oxygen much greater than the concentrations of electronic defects in UO_2 of ideal composition. Approximately then

$$x \cong X_O \cong \tfrac{1}{2} X_p \tag{11}$$

Substitution in eqn. (5) yields

$$x = X_O = (K_2/4)^{1/6} p_{O_2}^{1/6} \tag{12}$$

The excess of oxygen should under these assumptions be proportional to the 1/6 power of the ambient oxygen pressure.

The foregoing relations may be compared with the experimental results. To this end, eqn. (10) is written as

$$\log p_{O_2} = 2 \log x - 2 \log (K_2/K_1) \tag{13}$$

and eqn. (12) as

$$\log p_{O_2} = 6 \log x - 2 \log (K_2/4) \tag{14}$$

By plotting log p_{O_2} as a function of log x, a slope of 2 or 6 should result if either of the foregoing relations is valid. The data shown in Fig. 5 are plotted in this

Table 5. The initial and final slopes of the log x *vs.* log p_{O_2} curves within the UO_{2+x} phase.

	800°C	900°C	1000°C	1100°C	1150°C	1200°C
Initial slope	1.1	1.1	1.3	1.5	1.4	1.4
Final slope	6.4	6.3	7.0	5.2	9.8	11

Table 6. The equilibrium constant K_2 and the concentrations of the positive holes X_p and excess electrons X_n near the saturation limit of the UO_{2+x} phase.

Temp. (°C)	x	$\log p_{O_2}$	$\log K_2$	K_2	X_p	X_n
800	0.16	−9.19	2.81	630	0.32	0.12
900	0.19	−7.42	2.15	140	0.38	0.098
1000	0.22	−6.13	1.53	34	0.44	0.064
1100	0.24	−4.35	0.92	8.3	0.48	0.032

way in Fig. 12. It is found that the initial slope for small values of x is about 1.1 to 1.5 but increases rapidly with x until near the saturation limit of the UO_{2+x} phase the slope is about 6 (Table 5). The two limiting cases are approached at least semiquantitatively, indicating the applicability of the mass action principle to correlate the significant variables under these conditions.

Eqn. (14), valid for large values of x, gives

$$\log K_2 = 3 \log x - \tfrac{1}{2} \log p_{O_2} + \log 4 \qquad (15)$$

With the help of this equation, one can solve for the equilibrium constant K_2 (Table 6). Under assumption $x = X_O$, one then obtains from eqn. (5) the concentration of positive holes, X_p, and from eqn. (3) the concentration of excess electrons, X_n (the necessary values for K_1 are calculated below). All values are listed in Table 6.

Similarly, eqn. (13) gives for small values of x

$$\log K_1 = \tfrac{1}{2} \log p_{O_2} - \log x + \log K_2 \qquad (16)$$

The values for the equilibrium constant K_1 are given in Table 7. In the same Table are recorded the concentrations of the electronic defects in UO_2 of ideal composition which, according to eqn. (3), are $X_p = X_n = K_1^{\frac{1}{2}}$. The concentrations of electronic defects in UO_2 of ideal composition indicate a large intrinsic electronic disorder which is relatively insensitive to temperature and thus to the equilibrium oxygen partial pressure of the surroundings in agreement with the conductivity measurements of Hauffe [26]. These showed a constant electronic conductivity independent of the oxygen partial pressure in the compound UO_2 at around 1050°C.

Table 7. The equilibrium constant K_1 and the concentrations of the electronic defects in UO_2 of ideal composition.

Temp. (°C)	x	$\log p_{O_2}$	$\log K_1$	K_1	$X_p = X_n$
800	0.04	−11.24	−1.41	0.039	0.20
900	0.04	− 9.95	−1.43	0.037	0.20
1000	0.04	− 8.95	−1.55	0.028	0.17
1100	0.04	− 8.25	−1.81	0.016	0.13

By plotting log K_2 *vs.* $1/T$ a nearly straight line is obtained with a slope of 9270. Thus the heat of reaction (4) is -84.8 kcal/mole O_2. This is of the same order of magnitude as the relative partial molar heat of solution of oxygen in UO_{2+x} obtained previously by plotting log p_{O_2} *vs.* $1/T$ at constant composition.

For reaction (2), the heat of reaction above 900°C is about -14 kcal/mole O_2 and below that temperature about zero, again indicating the insensitivity of the electronic disorder to external conditions.

In an essentially similar treatment of the nonstoichiometry in UO_2, Aronson and Belle [13] obtained also a fairly good correlation between the calculated and observed partial pressures of oxygen by using the principle of mass action.

Acknowledgement. This investigation has been supported by *Suomen atomienergianeuvottelukunta* (Finnish Atomic Energy Commission). Thanks are due to Prof. M. H. Tikkanen for provision of facilities of the Metallurgical Laboratory of the Institute of Technology, Otaniemi, Finland.

REFERENCES

1. Kiukkola, K. and Wagner, C. *J. Electrochem. Soc.* **104** (1957) 308.
2. Wagner, C. *U. S. At. Energy Comm.* **WAPD — 144** (1955).
3. Kiukkola, K. and Wagner, C. *J. Electrochem. Soc.* **104** (1957) 379.
4. Kingery, W. D., Pappis, J., Doty, M. E. and Hill, D. C. *J. Am. Ceram. Soc.* **42** (1959) 393.
5. Carter, R. E. *J. Am. Ceram. Soc.* **43** (1960) 448.
6. Grønvold, F. *J. Inorg. & Nuclear Chem.* **1** (1955) 357.
7. Hoekstra, H. R., Siegel, S., Fuchs, L. H. and Katz, J. J. *J. Phys. Chem.* **59** (1955) 136.
8. Blackburn, P. E. *J. Phys. Chem.* **62** (1958) 897.
9. Wagner, C. *J. Chem. Phys.* **21** (1953) 1819.
10. Belle, J. and Auskern, A. B. in Kingery, W. D. (Ed.) *Kinetics of High-Temperature Processes*, John Wiley & Sons, New York 1959, p. 44.
11. Himmel, L., Mehl, R. F. and Birchenall, C. E. *Trans. AIME* **197** (1953) 827.
12. Biltz, W. and Müller, H. *Z. anorg. u. allgem. Chem.* **163** (1927) 257.
13. Aronson, S. and Belle, J. *J. Chem. Phys.* **29** (1958) 151.
14. Willardson, R. K., Moody, J. W. and Goering, H. L. *J. Inorg. & Nuclear Chem.* **6** (1958) 19.
15. Wagner, C. *Thermodynamics of Alloys*, Addison-Wesley Press, Inc., Cambridge, Mass. 1952.
16. Coughlin, J. P. *U. S. Bur. Mines, Bull.* **542** (1954) 54.
17. Ackermann, R. J., Thorn, R. J., Alexander, C. and Tetenbaum, M. *J. Phys. Chem.* **64** (1960) 350.
18. Jones, W. M., Gordon, J. and Long, E. A. *J. Chem. Phys.* **20** (1952) 695.
19. Rossini, F. D., Wagman, D. D., Evans, E. H., Levine, S. and Jaffe, I. *Natl. Bur. Standards (U.S.), Circ.* **500** (1952).
20. Osborne, D. W., Westrum, Jr., E. F. and Lohr, H. R. *J. Am. Chem. Soc.* **79** (1957) 529.
21. Brewer, L. *Chem. Revs.* **52** (1953) 1.
22. Westrum, Jr., E. F. and Grønvold, F. *J. Am. Chem. Soc.* **81** (1959) 1777.
23. Huber, Jr., E. J., Holley, Jr., C. E. and Meierkord, E. H. *J. Am. Chem. Soc.* **74** (1952) 3406.
24. Kelley, K. K. *U. S. Bur. Mines, Bull.* **584** (1960).
25. Popov, M. M., Gal'chenko, G. L. and Senin, M. D. *Zhur. Neorg. Khim.* **3** (1958) 1734.
26. Hauffe, K. *Z. physik. Chem.* **B 48** (1941) 124.

Received July 26, 1961.